Title	Carbon dioxide capture at the molecular level
Author(s)	Iida, Kenji; Yokogawa, Daisuke; Ikeda, Atsushi; Sato, Hirofumi; Sakaki, Shigeyoshi
Citation	Physical Chemistry Chemical Physics (2009), 11(38): 8556-8559
Issue Date	2009-07
URL	http://hdl.handle.net/2433/86188
Right	c 2009 Royal Society of Chemistry. 許諾条件により本文は2010-08-01に公開.
Type	Journal Article
Textversion	author

Carbon Dioxide Capture at Molecular Level

Kenji Iida, Daisuke Yokogawa, Atsushi Ikeda,
Hirofumi Sato,* and Shigeyoshi Sakaki

Department of Molecular Engineering, Kyoto University,
Kyoto, 615-8510, Japan

Abstract

Carbon dioxide is recognized as a typical greenhouse gas and drastic reduction of CO_2 emissions from industrial process is becoming more and more important in relation to global warming. In fact, the reaction between monoethanolamine (MEA) and CO_2 in aqueous solution has been widely used for the removal from flue gases. In this study, the role of the interplay between solvent water and nitrogen (MEA) – carbon (CO_2) bond formation is discussed based on the molecular theory using RISM-SCF-SEDD, which is the hybrid method of quantum chemistry of solute and statistical mechanics of solvent.

1 Introduction

Carbon dioxide is recognized as a typical greenhouse gas and drastic reduction of CO_2 emissions from industrial process is becoming more and more important in relation to global warming. Aqueous amine systems have been widely used for the removal of CO_2 from flue gases and the following process operates in these systems:

$$CO_2 + NHR_2 \rightarrow CO_2NR_2^- + H^+. \quad (1)$$

Among several factors controlling the capability of the absorption, a molecular characteristic of the amine is of primary importance. To develop a more efficient system, understanding of the mechanism is indispensable. Monoethanolamine (MEA) is one of the representative substances utilized for such a purpose. Thanks to intensive experimental studies,[1–5] it becomes clear

*hirofumi@moleng.kyoto-u.ac.jp

that the rate-determining step of the process is the bond formation between amine nitrogen and CO_2 carbon.

$$CO_2 + NH_2CH_2CH_2OH \rightarrow CO_2\text{-}NH_2CH_2CH_2OH. \quad (2)$$

A theoretical approach is expected to offer precious information that is difficult to be accessed by experimental research. Several studies based on standard molecular orbital theory as well as molecular simulation have been reported.[6–8] However, interplay between aqueous water and the bond formation –which is nothing but the changing of electronic structure in MEA-CO_2 system– has not been studied so far though it is essential for addressing the heart of the capture. Therefore, a simultaneous treatment of quantum chemistry and ensemble of solvent molecules is necessary, namely only QM/MM or its equivalent theory can touch the essence of the process. An explicit treatment of solvent water is crucial to deal with hydrogen bonding that governs the intermolecular interaction.

In the present study, the reaction mechanism of this bond formation between MEA and CO_2 is investigated by means of RISM-SCF-SEDD.[9–11] Since reference interaction site model (RISM)[12,13] is a statistical mechanics for molecular liquids, wealth of information including solvation structure, free energy change can be obtained efficiently. RISM-SCF-SEDD, in which RISM is coupled with molecular orbital theory, is recognized as an alternative to QM/MM. One of the big differences is the capability to compute accurate free energy with reasonable computational time due to the advantage of RISM, allowing us to use highly sophisticated electronic structure theory cooperated with solvation effect. The emphasis is on the free energy that describes the system in reality, which is difficult to elucidate only by considering a few water molecules. Now, this combinational method can afford the heart of the mechanism of the reaction.

2 Method

RISM is a statistical mechanics theory for molecular liquids developed by Chandler and Andersen.[12] The theory was then extended to treat electrostatic interaction (XRISM) by Rossky and Hirata.[13] The main equation of the theory is as follows,

$$\boldsymbol{\rho}\mathbf{h}\boldsymbol{\rho} = \boldsymbol{\omega} * \mathbf{c} * \boldsymbol{\omega} + \boldsymbol{\omega} * \mathbf{c} * \boldsymbol{\rho}\mathbf{h}\boldsymbol{\rho}. \quad (3)$$

Here, '*' denotes convolution integral, $\boldsymbol{\rho}$ is number of density, $\boldsymbol{\omega}$ is intramolecular correlation function defining the molecular geometry. $\mathbf{h}$ and $\mathbf{c}$ are total and direct correlation function, respectively. In the present study very standard hyper-netted chain (HNC) closure was employed to solve the equation.

$$\begin{aligned} c_{\alpha s}(r) &= \exp\left[-\beta u_{\alpha s}(r) + \gamma_{\alpha s}(r)\right] - \gamma_{\alpha s}(r) - 1, \\ \gamma_{\alpha s}(r) &= h_{\alpha s}(r) - c_{\alpha s}(r), \end{aligned} \tag{4}$$

where $u_{\alpha s}(r)$ is interaction between site α and s, $h_{\alpha s}(r)$ and $c_{\alpha s}(r)$ correspond to the matrix element appearing in Eq. 3, and $\beta = 1/k_{\mathrm{B}}T$. Free energy of solvation ($\Delta\mu$) is then readily computed by using obtained $h_{\alpha s}(r)$ and $c_{\alpha s}(r)$.[14]

$$\Delta\mu = -\frac{\rho}{\beta}\sum_{\alpha s}\int \mathrm{d}\mathbf{r}\left[c_{\alpha s}(r) - \frac{1}{2}h_{\alpha s}^2(r) + \frac{1}{2}h_{\alpha s}(r)c_{\alpha s}(r)\right]. \tag{5}$$

Some selected features and advantages of RISM are summarized as following: (1) The theory provides adequate thermodynamic ensemble and is free from statistical error or so-called sampling problem. It deals with an infinite number of solvent molecules and requires no 'simulation box'. (2) Since it is written in algebraic equation, computational cost is dramatically reduced compared to standard molecular simulation method. (3) The inputs of the computation are the same as those of simulations, and the outputs are very similar, too.

In RISM-SCF,[9,10] total energy of the system is defined as,

$$\mathscr{A} = E_{\mathrm{solute}} + \Delta\mu, \tag{6}$$

where E_{solute} is total energy of the solute molecule described by standard *ab initio* molecular orbital theory, corresponding to MEA and/or CO_2 in the present study. By using variational principle, a set of equations describing solution system is obtained.[10] Hence, the electronic structure of the solute and solvation structure are obtained in a self-consistent manner. RISM-SCF has been successfully applied to a wide range of chemical reactions in solution. It is our intent here to only describe the brief summary of the theory and assume the readers' familiarity of RISM-SCF as well as the statistical mechanics of molecular liquids. Some examples of recent studies are found in Refs.[15–18] More lengthly discussions can be found in the literatures.[19–21]

3 Computational Detail

The distance between the carbon atom of CO_2 and the nitrogen atom of MEA was taken as the reaction coordinate (R_C) to focus on the bond-making process in the reaction. The geometry optimisation was carried out at B3LYP/6-311++G** level in gas phase under the restriction of C_s structure, in which CO_2 and N-C-C-O-H are in the same plane. This treatment was necessary to exclude trivial intramolecular hydrogen-bonding structure that is unstable in aqueous solution. In fact, even starting from a low symmetry structure at meta-stable state (**III**; see below), optimisation in aqueous solution leads to the same C_s structure. In C_s symmetry, there is another conformation in which CO_2 is perpendicular to the N-C-C-O-H plane. But its total energy was only slightly higher ($\simeq$ 0.1 kcal/mol) and the rotation about the axis of N(MEA)–C(CO_2) bond was virtually free. All the energy was evaluated with CCSD(T)/6-311++G**. The present basis set is considered among the best, especially in combination with the highly sophisticated CCSD(T) theory and its dependency seems to be negligible. Computations in aqueous solution phase were then carried out with the RISM-SCF-SEDD by GAMESS package[23] modified by us and PCM methods by Gaussian 03 program[24] with these gas-phase geometries. We have also performed the optimisation in aqueous solution and found that the structure were almost unchanged. The barrier height is only 0.4 kcal mol^{-1} less than that in gas phase. Note that the aqueous-solution geometry by PCM is also different, and thus we decided to use the gas phase geometry to exclude the contribution of the geometrical difference between our method and PCM with the aim of focusing on the interplay between bond formation and solvation effect. The Lennard-Jones parameters of the solute were taken from Refs.[25–28] and SPC-like water was assumed for the solvent.[29] All of them are summarized in Table 1. To compute the weight of resonance structure, Pipek-Mezey localization[30] was utilized to separate valence orbitals. Unfortunately, π orbital and lone-pair orbital at oxygen were mixed together and four equivalent localized orbitals were obtained. Hence, these four orbitals were chosen to evaluate the weights using the standard Löwdin-type operator.[31] Then the contributions from two lone-pair orbitals, corresponding to O^- C^{2+} O^-, were eliminated to represent the resonance structure.

4 Results and discussion

4.1 Free energy profile in aqueous solution

Figure 1 shows the energy profile along the reaction coordinate, R_{C}. CO_2 approaches to MEA from the right hand side of the figure. In gas phase, the energy is continuously decreasing as the reaction proceeds, then the stable structure is found at $R_{\mathrm{C}} = 3.0$ Å (**I**). Obviously it does not correspond to the capturing because of too long bond length as well as barrier-free approaches that are not consistent with experimental knowledge. The energy monotonically increases at shorter regions ($R_{\mathrm{C}} < 3.0$Å) due to the repulsive interaction derived from *Pauli*'s principle. In aqueous solution, energy profiles changes drastically. Besides the minimum at $R_{\mathrm{C}} \simeq 3.0$ Å corresponding to **I**, another meta-stable structure appears at $R_{\mathrm{C}} < 2.0$ Å(**III**), which is followed by a fast proton dissociation step to reach the final product. The barrier height from **I** to **III** calculated by RISM-SCF-SEDD is 6.9 kcal mol^{-1}, being slightly higher (2.7 kcal mol^{-1}) than by PCM. Presumably the difference comes from strong stabilization of **I** due to the hydrogen bonding that is properly treated in RISM-SCF-SEDD. Since the experimentally obtained data is the activation enthalpy $\Delta H^{\ddagger}$, the free energy change mentioned above should be converted as following,

$$\Delta H^{\ddagger} = \Delta G^{\ddagger} + T\Delta S^{\ddagger}, \tag{7}$$

where activation entropy $\Delta S^{\ddagger}$ was calculated by difference formula, and standard corrections such as zero point energy are taken into account. Our activation enthalpy $\Delta H^{\ddagger}$ is 9.3 kcal mol^{-1} (The zero point and vibration contribution: 0.8 kcal mol^{-1}), which is in good agreement with experimental results (11.2,[2] 9.8,[3] 11.7,[4] and 11.1[5] kcal mol^{-1}). Although the free energy profile and the activation enthalpy are obtained using one of the most accurate theoretical methods available at the present time, further calibration would be desired because the results may depend on Lennard-Jones parameters, basis sets, the closure and so on.

4.2 Resonance structure

MEA–CO_2 bonding complex is formed at $R = 1.6$ Å caused by the charge migration from MEA nitrogen to CO_2 carbon (C_{cdx}). The change of electronic

structure may be nicely analyzed in terms of resonance structure embedded in molecular orbital by using the recently developed analysis based on the second quantization of singlet-coupling.[31] Fig. 2 shows the dominative weight of CO_2 moiety both in gas and aqueous phases. Supposably, the largest contribution to the electronic structure contains one ionic bond and one double bond. The doubly ionic structure is also important and the sum of three main contributions (**2**, **4** and **5**) is about 60%. In isolated CO_2, the change in electronic structure is negligibly small upon transferring from gas phase to aqueous solution. However, the bond formation significantly affects the electronic structure: the contribution from **5** is especially enhanced more than 10% while the double bond character (**2**) is considerably reduced. This may be simply attributed to the change of bond angle, O–C–O. The angle changes from 177° (**I**) to 141° (**II**; R_C = 2.0 Å), suggesting that the π conjugation is substantially suppressed and electron tends to be isolated at oxygen atoms. In terms of molecular orbital, the change corresponds to the electron transfer from N lone pair to CO_2 π^* orbital. In fact, natural population charge of N changes as $-0.95|e| \rightarrow -0.68|e|$ and that of O_{cdx} as $-0.62|e| \rightarrow -0.83|e|$. The same trends can be found in the resonance structure on C$\cdots$N bond at **III**: 38%(C–N), 10%(C^+ N^-) and 37%(C^- N^+), respectively (corresponding gas phase values are 34%, 42%, 7%).

4.3 Solvation structure and solvation free energy change

Because of the large charge migration, solvation structure around them drastically changes as the reaction proceeds. Fig. 3 shows the change of pair correlation functions (PCFs). The left panel exhibits PCF between N and solvent-water hydrogen (H_W), while the right one is that between O_{cdx}-H_W. The sharp peaks found at r = 2.0 Å in both panels correspond to hydrogen bonding. At first, MEA is weakly hydrated around N atom at **I**, and the peak completely disappears in the transition state (**II**). This is, of course, caused by the steric hindrance by approaching CO_2 and the solvation structure hardly changes after passing through **T**. PCF around CO_2 oxygen also shows weak hydrogen bonding at **I**, but the peak is contrastively increasing as the reaction proceeding, indicating that CO_2 moiety strongly attracts solvent water even at $R_C < 2.0$ Å. The development of hydrogen bonding is attributed to the above mentioned increasing of O_{cdx} charge.

Both of these changes in hydration structure affect the free energy change in this bond-forming region. Solvation free energy $\Delta\mu$ (Eq.5) can be "for-

mally" divided into the contribution from each atom labeled α.

$$\Delta\mu = \sum_{\alpha} \Delta\mu_{\alpha}, \tag{8}$$

and

$$\Delta\mu_{\alpha} = -\frac{\rho}{\beta} \sum_{s} \int \mathrm{d}\mathbf{r} \left[c_{\alpha s}(r) - \frac{1}{2} h_{\alpha s}^{2}(r) + \frac{1}{2} h_{\alpha s}(r) c_{\alpha s}(r) \right]. \tag{9}$$

This quantity represents how much the contribution from each site is. Fig. 4 shows the change of total solvation free energy ($\Delta\mu_{total}$) and the main elements, $\Delta\mu_{total}$, $\Delta\mu_{\mathrm{N}}$ and $\Delta\mu_{\mathrm{O_{cdx}}}$, along R_{C}. $\Delta\mu_{\mathrm{N}}$ increases along the reaction coordinate from I to III region, whereas $\Delta\mu_{\mathrm{O_{cdx}}}$ decreases around the same region. Namely, while $\mathrm{O_{cdx}}$ is solvated, a nitrogen atom is desolvated as the reaction proceeds. At the region from **I** to **II**, the hydration-development around $\mathrm{O_{cdx}}$ and de-hydration around N are virtually canceled out, and thus the total free energy change in aqueous solution eventually looks very similar to the energy change in the gas phase. However, at the region from **II** to **III**, $\mathrm{O_{cdx}}$ hydration becomes dominative and the total free energy decreases to establish the meta-stable intermediate. These are consistent with the change of the solvation structure. In other words, the barrier and stability of the state in aqueous solution are understood as an interplay of the dehydration around N and hydration around $\mathrm{O_{cdx}}$. Note that many previous works indicate that a proton is released from this meta-stable intermediate as the second step of the absorption.

4.4 Conclusion

In summary, we first report the bonding mechanism between carbon dioxide and monoethanolamine at molecular level. In gas phase, an ordinary single minimum is formed at $R_{\mathrm{C}} = 3.0$ Å without barrier. On the other hand, in aqueous solution, after the formation of intermediates similar to the gas phase, a stable structure is found at the bonding region ($R_{\mathrm{C}} = 1.6$ Å) *via* the transition state at $R_{\mathrm{C}} = 2.0$ Å with activation enthalpy of 9.3 kcal/mol, which shows good agreement with experimental knowledge. The hybrid method that can describe both electronic structure change and hydrogen bonding is a promising tool to understand the CO_2 capture. This understanding would lead to a more tactical search for amines with higher absorption capability.

Acknowledgement

This work has been financially supported by the Grant-in Aids (19350010, 20550013, 452-20031014 and 461), all supported by the Ministry of Education, Culture, Sports, Science and Technology (MEXT) Japan. The authors thank to Dr. Yukihiko Inoue for drawing their attention to the importance of this subject.

References

[1] P. D. Vaidya, E. Y. Kenig, *Chem. Eng. Tech.*, 2007, **30**, 1467.

[2] E. Alper, *Ind. Eng. Chem. Res.*, 1990, **29**, 1725.

[3] H. Hikita, S. Asai, H. Ishikawa, M. Honda, *Chem. Eng. J.*, 1977, **13**, 7.

[4] J. E. Crooks, J. P. Donnellan, *J. Chem. Soc. Perkin. Trans. 2*, 1989, **4**, 331.

[5] S. H. Ali, *Int. J. Chem. Kinet*, 2005, **37**, 391.

[6] E. F. da Silva, H. F. Svendsen, *Ind. Eng. Chem. Res.*, 2004, **43**, 3413.

[7] E. F. da Silva, T. Kuznetsova, B. Kvamme, K. M. Merz Jr., *J. Phys. Chem. B*, 2007, **111**, 3695.

[8] B. Arstad, R. Blom, O. Swang, *J. Phys. Chem. A*, 2007, **111**, 1222.

[9] S. Ten-no, F. Hirata, S. Kato, *J. Chem. Phys.*, 1994, **100**, 7443.

[10] H. Sato, F. Hirata, S. Kato, *J. Chem. Phys.*, 1996, **105**, 1546.

[11] D. Yokogawa, H. Sato, S. Sakaki, *J. Chem. Phys.*, 2007, **126**, 244504.

[12] H. C. Andersen, D. Chandler, *J. Chem. Phys.*, 1972, **57**, 1930.

[13] F. Hirata, P. J. Rossky, *Chem. Phys. Lett.*, 1981, **83**, 329.

[14] S. J. Singer, D. Chandler, *Mol. Phys.*, 1985, **55**, 621.

[15] H. Sato, S. Sakaki, *J. Phys. Chem. A*, 2004, **108**, 1629.

[16] N. Minezawa, S. Kato, *J. Phys. Chem. A*, 2005, **109**, 5445.

[17] K. Iida, D. Yokogawa, S. Sato, S. Sakaki, *Chem. Phys. Lett.*, 2007, **443**, 264.

[18] S. Hayaki, D. Yokogawa, S. Sato, S. Sakaki, *Chem. Phys. Lett.*, 2008, **458**, 329.

[19] *Continuum Solvation Models in Chemical Physics*, eds. B. Mennucci and R. Cammi, John Wiley & Sons, Chichester, 2007.

[20] *Molecular Theory of Solvation, Understanding Chemical Reactivity*, ed. F. Hirata, Springer, 2003.

[21] *Computational Biochemistry and Biophysics*, eds. O. M. Becker, A. D. MacKerell, Jr., B. Roux and K. Watanabe, Marcel Dekker, New York, 2001.

[22] J. Tomasi, B. Mennucci, R. Cammi, *Chem. Rev.*, 2005, **105**, 2999.

[23] M. W. Schmidt, K. K. Baldridge, J. A. Boatz, S. T. Elbert, M.S. Gordon, J. H. Jensen, S. Koseki, N. Matsunaga, K. A. Nguyen, S. Su, T. L. Windus, M. Dupuis, J. A. Montgomery, *J. Comput. Chem.*, 1993, **14**, 1347.

[24] Gaussian 03, Revision C.02; Gaussian Inc., Wallingford, CT, 2004.

[25] R. C. Rizzo, W. L. Jorgensen, *J. Am. Chem. Soc.*, 1999, **121**, 4827.

[26] W. L. Jorgensen, *J. Phys. Chem.*, 1986, **90**, 1276.

[27] S.J. Weiner, P.A. Kollman, D.A. Case, U.C. Singh, C. Ghio, G. Alagona, S. Profeta, Jr, P. Weiner, *J. Am. Chem. Soc.*, 1984, **106**, 765.

[28] S.J. Weiner, P.A. Kollman, D.T. Nguyen, D.A. Case, *J. Comput. Chem.*, 1986, **7**, 230.

[29] H. J. C. Berendsen, J. P. M. Postma, W. F. van Gunsteren, J. Hermans, in *Intermolecular Forces*, ed. B. Pullman, Reidel, Dordrecht, 1981.

[30] J. Pipek and P. G. Mezey, *J. Chem. Phys.*, 1989, **90**, 4916.

[31] (a) A. Ikeda, Y. Nakao, H. Sato, S. Sakaki, *J. Phys. Chem. A*, 2006, **110**, 9028. (b) A. Ikeda, D. Yokogawa, H. Sato, S. Sakaki, *Chem. Phys. Lett.*, 2006, **424**, 499. (c) A. Ikeda, D. Yokogawa, H. Sato, S. Sakaki, *Int. J. Quantum Chem.*, 2007, **107**, 3132. (d) A. Ikeda, Y. Nakao, H. Sato, S. Sakaki, *J. Chem. Theor. Comp.*, in press.

Table 1: Lennard-Jones parameters.

	σ /Å	ϵ /kcal mol^{-1}
	Solute	
N	3.300	0.170
C(methyl)	3.500	0.066
C(CO_2)	3.296	0.120
O(OH)	3.070	0.170
O(CO_2)	2.850	0.200
H(methyl)	2.500	0.030
H(HO)	1.000	0.0560
	Solvent	
O	3.166	0.1550
H	1.000	0.0560

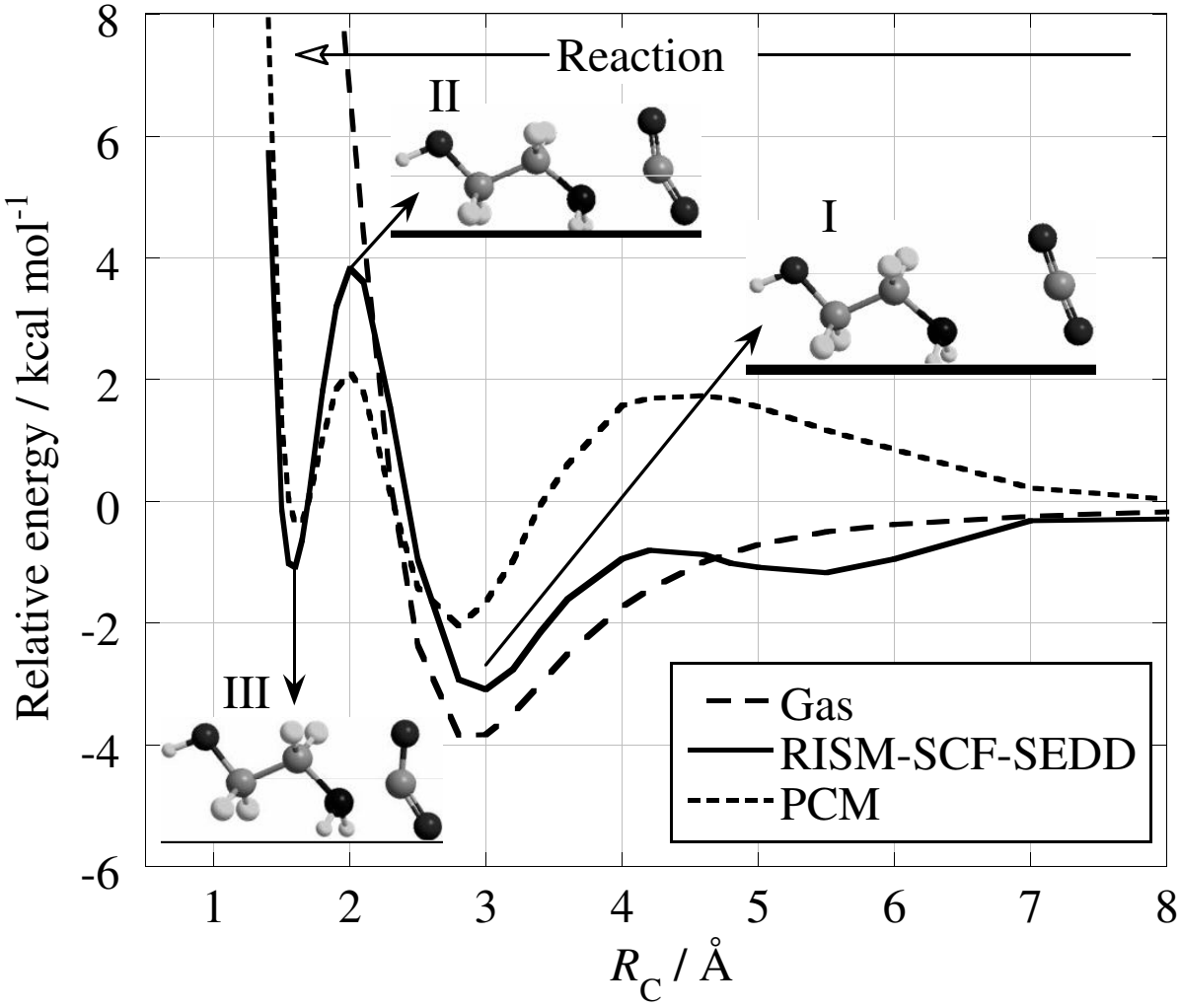

Figure 1: Potential energy curve for the C–N bond formation in gas phase (dashed line) and free energy curves in aqueous solution calculated by RISM-SCF-SEDD (solid line) and PCM (dotted line) along the reaction coordinate (R_C). The inset structures are at R_C = 3.0 Å (I), 2.0 Å (II), 1.6 Å (III), respectively.

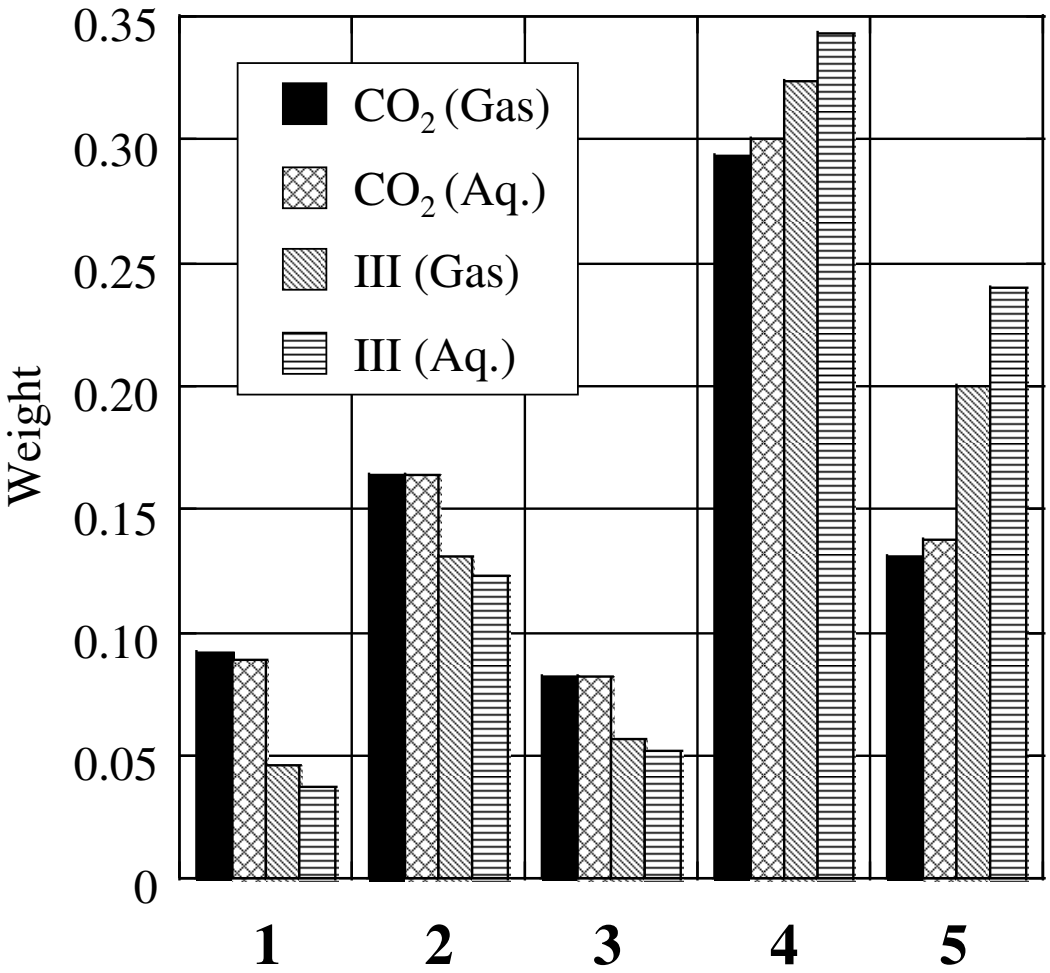

Figure 2: Change of selected resonance Weights of CO_2 moiety from the isolated state (CO_2) to the complex. **1**: O=C$^-$ $\equiv$O$^+$, **2**: O=C=O, **3**: O$^-$C$\equiv$O$^+$, **4**: O$^-$$-C^+$ =O, **5**: O$^-$$-C^{2+}-O^-$. Note that symmetrically equivalent contributions are summed up, *e.g.*, **4** comprises both of O$^-$$-C^+$ =O and O=C$^+$$-O^-$.

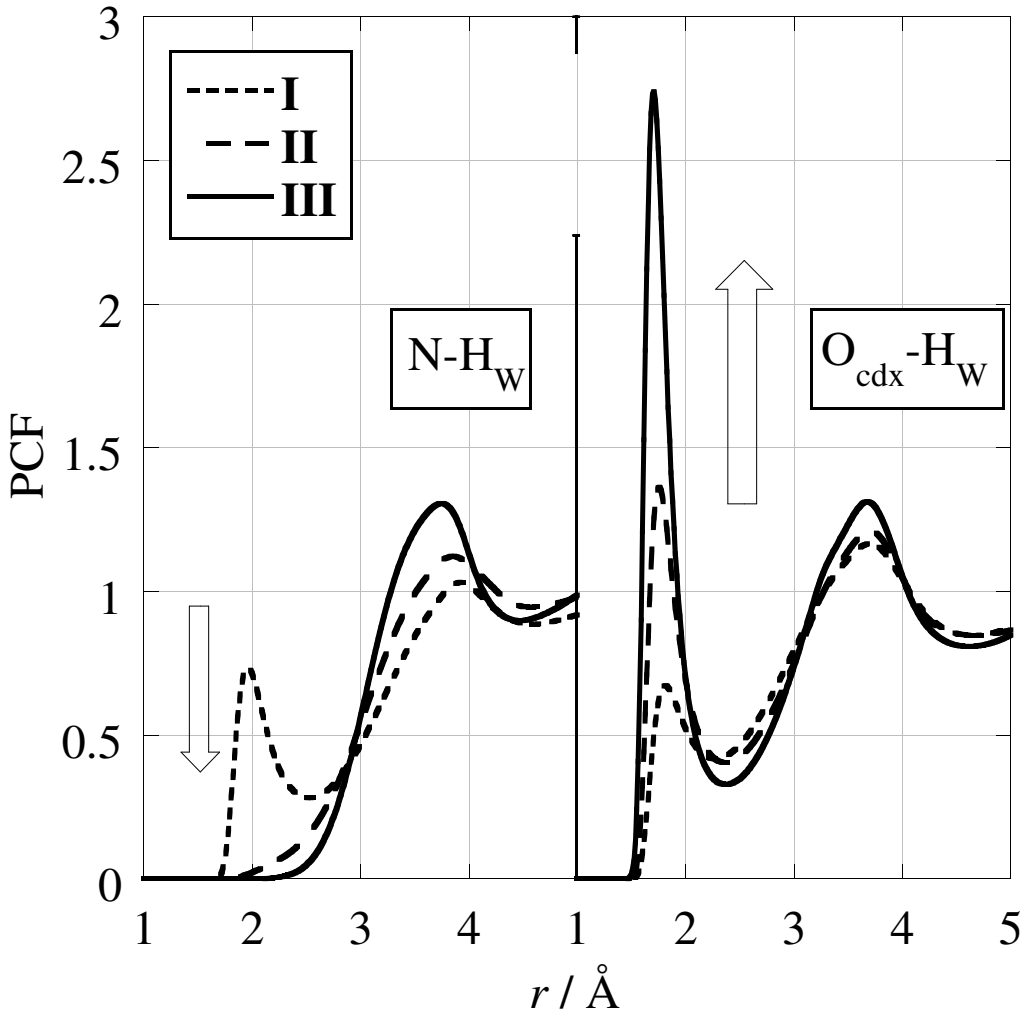

Figure 3: Pair correlation function of N-H_W (left side) and O_{cdx}-H_W (right side) of R_C=3.0 Å (I, dotted line), R_C=2.0 Å (II, dashed line), and R_C=1.6 Å (III, solid line).

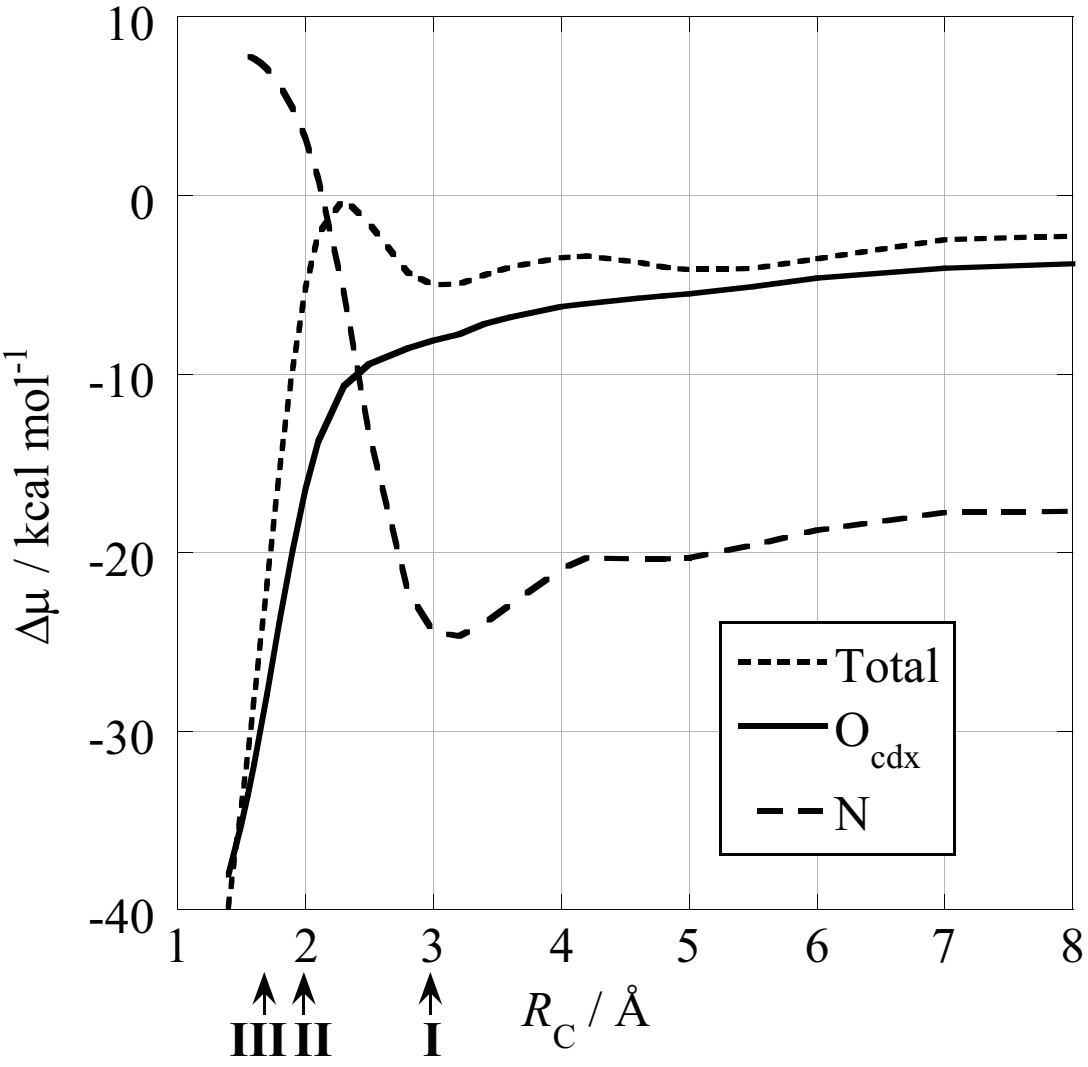

Figure 4: Selected solvation free energy components along R_{C} calculated by RISM-SCF-SEDD.